Dalton Transactions

PAPER

View Article Online
View Journal | View Issue

Cite this: *Dalton Trans.*, 2015, **44**, 15250

Introduction of luminescent rhenium(I), ruthenium(II), iridium(III) and rhodium(III) systems into rhodamine-tethered ligands for the construction of bichromophoric chemosensors†

Chunyan Wang,[a,b] Ho-Chuen Lam,[b] Nianyong Zhu[b] and Keith Man-Chung Wong*[a,b]

Received 13th February 2015,
Accepted 21st April 2015

DOI: 10.1039/c5dt00661a

www.rsc.org/dalton

Several classes of luminescent transition metal complexes, including rhenium(I) tricarbonyl diimine, ruthenium(II) diimine, cyclometallated iridium(III) and rhodium(III) diimine, as well as ruthenium(II) and iridium(III) terpyridine systems, tethered with rhodamine moieties, have been synthesized and characterized. The X-ray crystal structure of one cyclometallated rhodium(III) diimine (**11**) with a rhodamine pendant was determined. Most of the complexes were found to exhibit emission in fluid solution at room temperature. Depending on the nature of the transition metal system, the emission origin was mainly assigned to be derived from the triplet excited state of the metal-to-ligand charge transfer (^{3}MLCT) or the intraligand (^{3}IL) transition. The cation-binding properties of these complexes toward various cations were investigated by electronic absorption and emission spectroscopy. Some of them were found to exhibit new low-energy absorption and emission bands, attributed to the ring opening of the rhodamine moiety, with high selectivity and/or high sensitivity for various cations, in agreement with sensing and spectroscopic behaviours of the rhodamine derivative. Depending on the nature of the transition metal centres, the chelating ligands as well as the linker to the rhodamine derivative, different sensing properties in terms of selectivity, sensitivity and binding stability, could be obtained.

Introduction

Host–guest chemistry based on macromolecules has gained importance since the pioneering work on crown ethers, cryptands, and spherands by Pedersen, Lehn and Cram.[1] This research area can help in elucidating the factors that control receptor–substrate interactions in biological systems, and can also lead to the creation of novel compounds and invention of novel chemical processes. Achieving high selectivity for the analyte of interest over a complex background of potentially competing compounds is a challenging task in sensor development. In order to achieve selectivity towards target cations, the design and synthesis of new macrocyclic ligands with different cavity sizes, donor atom types, ring substituents, and so on, have resulted in a large number and variety of compounds. Calix[*n*]arenes[2] are one example representing a family of selective ion receptors, owing to their unique molecular structure with pre-defined conformations and pre-organized geometries. It is also known that incorporating some soft donor atoms such as sulfur into the crown ether moieties may also tune their selective binding ability for transition metal ions.[3]

In view of the superior spectroscopic properties of rhodamine derivatives, which were found to exist in ring-opened and ring-closed forms with very distinctive colours and emission behaviours, utilizing such class of compounds in the corresponding chemosensing with high selectivity and sensitivity has aroused tremendous interest.[4–13] Numerous rhodamine-based selective Hg^{2+} chemosensors have been reported by different research groups.[6–8] Based on such a rhodamine-based spirolactam system, other new selective fluorescent sensors to sense Fe^{3+},[7c–e,8] Cu^{2+},[9] Cr^{3+},[7d,11] and Au^{3+},[12] have been demonstrated. Some of the rhodamine-based derivatives have also been explored as selective chemosensors for the detection of nucleic acids,[13a] hydrogen peroxide and glucose,[13b] peroxynitrite,[13c] nitric oxide[13d] and hypochlorous acid.[13e] Apart from some rhodamine systems, in which the sensing mechanism involves an irreversible chemical reaction, the selectivity towards certain analytes in an equilibrium is not

[a]*Department of Chemistry, South University of Science and Technology of China, No. 1088, Tangchang Boulevard, Nanshan District, Shenzhen 518055, Guangdong, P.R. China*

[b]*Department of Chemistry, The University of Hong Kong, Pokfulam Road, Hong Kong, China. E-mail: keithwongmc@sustc.edu.cn*

†Electronic supplementary information (ESI) available: Photophysical spectra, and other electronic absorption and emission spectral changes upon the addition of various metal cations. X-ray crystallographic data for **11** in CIF format. CCDC 1046703. For ESI and crystallographic data in CIF or other electronic format see DOI: 10.1039/c5dt00661a

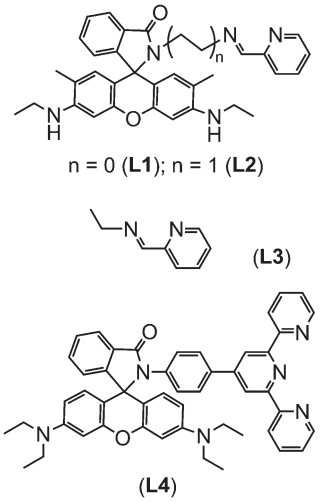

$Re(CO)_3$(**L1**)Br	(**1**)	$[Ir(ppy)_2$(**L1**)$]PF_6$	(**7**)
$Re(CO)_3$(**L2**)Br	(**2**)	$[Ir(ppy)_2$(**L2**)$]PF_6$	(**8**)
$Re(CO)_3$(**L3**)Br	(**3**)	$[Ir(ppy)_2$(**L3**)$]PF_6$	(**9**)
$[Ru(bpy)_2$(**L1**)$](PF_6)_2$	(**4**)	$[Rh(ppy)_2$(**L1**)$]PF_6$	(**10**)
$[Ru(bpy)_2$(**L2**)$](PF_6)_2$	(**5**)	$[Rh(ppy)_2$(**L2**)$]PF_6$	(**11**)
$[Ru(bpy)_2$(**L3**)$](PF_6)_2$	(**6**)	$[Rh(ppy)_2$(**L3**)$]PF_6$	(**12**)
$[Ru(terpy)$(**L4**)$](PF_6)_2$	(**13**)		
$[Ir(terpy)$(**L4**)$](PF_6)_3$	(**14**)		

Scheme 1 Ligands **L1**–**L4** and complexes **1**–**14**.

well-known. The nature of the pendant group tethered to the rhodamine moiety and the linker between them as well as the number and type of heteroatoms in the pendant are anticipated to influence the sensitivity and selectivity of the sensing properties.

Our group has recently reported a novel system of a bichromophoric chemosensor as the first example, with hybridization of the organic fluorogenic rhodamine sensing derivative and the luminescent cyclometallated iridium-(III) complex.[8a,c] Interestingly, the energy-transfer process from rhodamine 6G to the iridium(III) luminophore could be modulated through the selective Hg^{2+} ion binding upon ring opening of rhodamine 6G. As an extension on the related bichromophoric systems with the combination of various transition metal complexes and rhodamine-derivatives, we herein report the synthesis and characterization of several classes of luminescent transition metal complexes, including rhenium(I) tricarbonyl diimine, ruthenium(II) diimine, cyclometallated iridium(III) and rhodium(III) diimine, and ruthenium(II) and iridium(III) terpyridine systems, tethered with rhodamine moieties (Scheme 1). Their photophysical and cation-binding properties have been investigated. The sensing behaviours, such as selectivity, sensitivity and binding stability, were correlated with the structural combination of the nature of the transition metal centres, chelating ligands as well as the linker to the rhodamine derivative.

Experimental section

Materials and reagents

All the solvents for synthesis were of analytical grade. Methanol and acetonitrile for analysis were of HPLC grade. Rhodamine 6G, rhodamine B base, ethylamine and phosphorus oxychloride were purchased from the Acros Organics Company. 2-Pyridinecarboxaldehyde, 2,2′:6′,2″-terpyridine, iridium(III) chloride hydrate, ruthenium(III) chloride hydrate and ammonium hexafluorophosphate were purchased from the Aldrich Chemical Company. Rhenium(I) pentacarbonyl bromide was purchased from Strem Chemicals, Inc. Mercury(II) perchlorate, lead(II) perchlorate, copper(II) perchlorate, zinc(II) perchlorate, cadmium(II) perchlorate, barium(II) perchlorate, manganese(II) perchlorate, silver(I) perchlorate, potassium(I) perchlorate, sodium(I) perchlorate and lithium(I) perchlorate were purchased from the Aldrich Chemical Company with purities over 99.0%, and were used as received. Hydrazine monohydrate, ethylenediamine, triethylamine and potassium hexafluorophosphate were purchased from the Alfa Aesar Company. 2,2′-Bipyridine was purchased from Lacaster Synthesis Ltd. The precursors rhodamine 6G hydrazide,[13c] rhodamine 6G ethylamine,[6c] 4′-(4-amino-phenyl)-2,2′:6′,2″-terpyridine,[14] $Ir_2(ppy)_4Cl_2$,[15] $Rh_2(ppy)_4Cl_2$,[15,16] $Ru(bpy)_2Cl_2$,[17] $Ru(terpy)Cl_3$ [18] and $Ir(terpy)Cl_3$ [19] (ppy = 2-phenylpyridine, bpy = 2,2′-bipyridine, terpy = 2,2′:6′,2″-terpyridine) were synthesized according to literature methods.

Synthesis

L1. This was prepared using the modification of a reported procedure.[20] A solution of rhodamine 6G hydrazide (0.50 g, 1.17 mmol) and 2-pyridinecarboxaldehyde (0.13 ml, 1.34 mmol) in methanol (40 ml) was heated to reflux under N_2 for 3 h. The solvent was removed under reduced pressure. Subsequent recrystallization by vapour diffusion of diethyl ether into a dichloromethane solution of the product gave **L1** as pale pink crystals. Yield: 0.38 g, 63%. ^{1}H NMR (400 MHz, $CDCl_3$, 298 K, relative to $SiMe_4$)/ppm: δ 8.44–8.46 (m, 1H, pyridyl H), 8.24 (s, 1H, N=CH), 7.97–8.05 (m, 2H, rhodamine ArH and pyridyl H), 7.56–7.62 (m, 1H, pyridyl H), 7.43–7.51 (m, 2H, rhodamine ArH), 7.10–7.14 (m, 1H, pyridyl H), 7.04–7.07 (m, 1H, rhodamine ArH), 6.41 (s, 2H, xanthene H), 6.35 (s, 2H, xanthene H), 3.48–3.51 (m, 2H, NH), 3.16–3.20 (m, 4H, N–CH_2–CH_3), 1.86 (s, 6H, CH_3 on xanthene ring), 1.32 (t, J =

6.5 Hz, 6H, N–CH_2–CH_3). ^{13}C NMR (100 MHz, $CDCl_3$, 298 K, relative to $SiMe_4$)/ppm: δ 165.66, 154.51, 152.92, 149.06, 147.68, 145.52, 136.11, 133.93, 128.34, 127.78, 127.38, 123.74, 123.71, 123.65, 120.62, 118.11, 105.83, 97.19, 65.82, 38.42, 16.81, 16.80, 14.84. Positive FAB-MS: m/z 517 $[M]^+$.

L2. This was prepared by a method similar to that of **L1** except rhodamine 6G ethylamine (0.58 g, 1.17 mmol) was used instead of rhodamine 6G hydrazide. **L2** was isolated as a pale orange solid. Yield: 0.43 g, 68%. ^{1}H NMR (300 MHz, $CDCl_3$, 298 K, relative to $SiMe_4$)/ppm: δ 8.57 (d, J = 4.8 Hz, 1H, pyridyl H), 8.05 (s, 1H, N=CH), 7.94 (d, J = 5.8 Hz, 1H, rhodamine ArH), 7.82 (d, J = 8.0 Hz, 1H, pyridyl H), 7.67 (t, J = 8.0 Hz, 1H, pyridyl H), 7.42–7.45 (m, 2H, rhodamine ArH), 7.25–7.27 (m, 1H, pyridyl H), 7.03 (d, J = 7.9 Hz, 1H, rhodamine ArH), 6.33 (s, 2H, xanthene H), 6.24 (s, 2H, xanthene H), 3.42–3.54 (m, 6H, NH + NCH_2CH_2N), 3.15–3.23 (m, 4H, NH–CH_2–CH_3), 1.86 (s, 6H, CH_3 on xanthene ring), 1.32 (t, J = 7.1 Hz, 6H, N–CH_2–CH_3. ^{13}C NMR (100 MHz, $CDCl_3$, 298 K, relative to $SiMe_4$)/ppm: δ 161.99, 156.79, 154.03, 151.86, 149.86, 147.50, 141.23, 136.89, 132.54, 128.68, 128.58, 127.00, 123.92, 122.88, 120.80, 117.99, 106.20, 96.76, 65.20, 59.27, 41.42, 38.49, 16.81, 14.87. Positive FAB-MS: m/z 545 $[M]^+$.

L3. A mixture of 2-pyridinecarboxaldehyde (6 ml, 0.06 mol) and ethylamine (7 ml, 0.13 mol) was stirred in an ice-water bath for 2 h and then at room temperature for another 2 h. The yellow reaction mixture was then extracted three times with diethyl ether. The combined extracts were dried over anhydrous $MgSO_4$, filtered and evaporated to dryness to afford **L3** as a yellow liquid. Yield: 6.9 g, 82%. ^{1}H NMR (400 MHz, $CDCl_3$, 298 K, relative to $SiMe_4$)/ppm: δ 8.55 (dd, J = 1.6 and 4.4 Hz, 1H, pyridyl H), 8.31 (s, 1H, N=CH), 7.90 (d, J = 8.0 Hz, 1H, pyridyl H), 7.65 (td, J = 1.6 and 8.0 Hz, 1H, pyridyl H), 7.22 (td, J = 1.6 and 4.4 Hz, 1H, pyridyl H), 3.63 (q, J = 7.3 Hz, 2H, CH_2), 1.24 (t, J = 7.3 Hz, 3H, CH_3). ^{13}C NMR (100 MHz, $CDCl_3$, 298 K, relative to $SiMe_4$)/ppm: δ 161.27, 154.59, 149.36, 136.47, 124.55, 121.15, 55.61, 16.02. Positive EI-MS: m/z 134 $[M]^+$.

L4. A mixture of the rhodamine B base (0.51 g, 1.15 mmol) and 4′-(4-amino-phenyl)-2,2′:6′,2″-terpyridine (0.37 g, 1.15 mmol) in the presence of $POCl_3$ (0.11 ml, 1.21 mmol) and Et_3N (0.17 ml, 1.21 mmol) in dry 1,2-dichloroethane (20 ml) was heated to reflux for 24 h. The solvent was then removed under reduced pressure. The dark purple residue was dissolved in dichloromethane, and the solution was washed three times with saturated sodium hydrogen carbonate and then three times with deionized water. The organic layer was dried over anhydrous $MgSO_4$, filtered and evaporated to dryness. Subsequent recrystallization by vapour diffusion of diethyl ether into a dichloromethane solution of the product gave **L4** as pale purple crystals. Yield: 0.53 g, 61%. ^{1}H NMR (300 MHz, $CDCl_3$, 298 K, relative to $SiMe_4$)/ppm: δ 8.62–8.68 (m, 6H, terpyridyl H), 8.01–8.04 (m, 1H, rhodamine ArH), 7.85 (t, J = 6.2 Hz, 2H, terpyridyl H), 7.69 (d, J = 8.4 Hz, 2H, phenyl H on terpyridine), 7.49–7.51 (m, 2H, rhodamine ArH), 7.32 (t, J = 6.2 Hz, 2H, terpyridyl H), 7.16–7.18 (m, 1H, rhodamine ArH), 7.04 (d, J = 8.4 Hz, 2H, phenyl H on terpyridine), 6.66 (d, J = 8.3 Hz, 2H, xanthene H), 6.25–6.34 (m, 4H, xanthene H), 3.33 (q, J = 7.1 Hz, 8H, N–CH_2–CH_3), 1.16 (t, J = 7.1 Hz, 12H, N–CH_2–CH_3). ^{13}C NMR (100 MHz, $CDCl_3$, 298 K, relative to $SiMe_4$)/ppm: δ 167.99, 156.35, 155.91, 153.64, 153.16, 149.75, 149.20, 148.96, 138.04, 136.95, 136.01, 133.12, 130.81, 128.85, 128.28, 127.56, 126.99, 124.13, 123.89, 123.53, 121.42, 118.72, 108.22, 106.32, 97.92, 67.71, 44.46, 12.79. Positive FAB-MS: m/z 748 $[M]^+$.

Re(L1)(CO)$_3$Br (1). This was synthesized using the modification of a literature procedure.[20,21] A mixture of $Re(CO)_5Br$ (0.07 g, 0.17 mmol) and **L1**(0.09 g, 0.17 mmol) in toluene (20 ml) was heated to reflux under N_2 for 6 h. The solvent was removed under reduced pressure. Subsequent recrystallization by vapour diffusion of diethyl ether into a dichloromethane solution of the product gave **1** as red-orange crystals. Yield: 0.10 g, 66%. ^{1}H NMR (300 MHz, $CDCl_3$, 298 K, relative to $SiMe_4$)/ppm: δ 8.94 (d, J = 5.67 Hz, 1H, pyridyl H), 8.09–8.12 (m, 2H, N=CH + rhodamine ArH), 7.80 (t, J = 7.7 Hz, 1H, pyridyl H), 7.53–7.55 (m, 2H, rhodamine ArH), 7.32–7.40 (m, 2H, pyridyl H), 7.00–7.03 (m, 1H, rhodamine ArH), 6.53 (s, 1H, xanthene H), 6.41 (s, 1H, xanthene H), 6.37 (s, 1H, xanthene H), 6.30 (s, 1H, xanthene H), 3.55–3.61 (m, 2H, NH), 3.14–3.26 (m, 4H, N–CH_2–CH_3), 1.91–1.94 (m, 6H, CH_3 on xanthene ring), 1.27–1.35 (m, 6H, N–CH_2–CH_3). ^{13}C NMR (100 MHz, $(CD_3)_2CO$, 298 K, relative to $SiMe_4$)/ppm: δ 198.30, 197.43, 188.53, 163.94, 158.46, 153.75, 153.59, 152.92, 152.60, 152.20, 149.88, 149.75, 140.36, 135.39, 130.32, 129.76, 129.72, 128.89, 128.18, 128.16, 124.59, 124.16, 120.50, 120.27, 105.04, 103.62, 97.18, 96.73, 71.24, 38.77, 38.75, 17.29, 17.21, 14.62, 14.59, 14.55, 14.52. Positive FA B-MS: m/z 868 $[M]^+$. Anal. calc. for $C_{35}H_{31}BrN_5O_5Re\cdot\frac{1}{2}H_2O$: C, 47.95; H, 3.68; N, 7.99. Found: C, 47.94; H, 3.85; N, 7.65.

Re(L2)(CO)$_3$Br (2). This was prepared by a method similar to that of **1** except **L2** (0.10 g, 0.17 mmol) was used instead of **L1**. Complex **2** was isolated as orange crystals. Yield: 0.11 g, 71%.^{1}H NMR (300 MHz, $CDCl_3$, 298 K, relative to $SiMe_4$)/ppm: δ 8.97 (d, J = 4.7 Hz, 1H, pyridyl H), 8.44 (s, 1H, N=CH), 7.91–8.01 (m, 2H, rhodamine ArH + pyridyl H), 7.76 (d, J = 7.8 Hz, 1H, pyridyl H), 7.47–7.53 (m, 3H, rhodamine ArH + pyridyl H), 7.10–7.13 (m, 1H, rhodamine ArH), 6.38 (s, 2H, xanthene H), 6.22 (s, 1H, xanthene H), 6.17 (s, 1H, xanthene H), 3.76–3.92 (m, 2H, NH), 3.51–3.68 (m, 4H, NCH_2CH_2N), 3.18–3.27 (m, 4H, N–CH_2–CH_3), 1.90–1.92 (m, 6H, CH_3 on xanthene ring), 1.34–1.36 (m, 6H, N–CH_2–CH_3). ^{13}C NMR (100 MHz, $CDCl_3$, 298 K, relative to $SiMe_4$)/ppm: δ 196.85, 195.10, 185.84, 168.36, 166.99, 155.24, 153.23, 153.20, 152.17, 152.10, 147.96, 147.91, 138.84, 133.05, 131.04, 128.47, 128.41, 128.29, 128.18, 128.07, 124.18, 123.09, 118.57, 118.24, 106.02, 105.35, 96.97, 96.82, 77.36, 65.46, 63.22, 40.05, 38.50, 17.00, 16.91, 14.84, 14.83. Positive FAB-MS: m/z 896 $[M]^+$. Anal. calc. for $C_{37}H_{35}BrN_5O_5Re$: C, 49.44; H, 4.26; N, 7.79. Found: C, C, 49.32; H, 3.98; N, 7.75.

Re(L3)(CO)$_3$Br (3). This was prepared by a method similar to that of **1** except **L3** (0.03 g, 0.25 mmol) was used instead of **L1**. Complex **2** was isolated as orange-yellow crystals. Yield: 56.1 mg, 66%. ^{1}H NMR (300 MHz, $CDCl_3$, 298 K, relative to $SiMe_4$)/ppm: δ 9.05 (d, J = 5.1 Hz, 1H, pyridyl H), 8.74 (s, 1H,

N═CH), 8.05 (t, J = 8.3 Hz, 1H, pyridyl H), 7.91 (d, J = 7.6 Hz, 1H, pyridyl H), 7.55 (t, J = 5.8 Hz, 1H, pyridyl H), 3.33 (q, J = 7.1 Hz, 2H, CH_2), 1.16 (t, J = 7.1 Hz, 3H, CH_3). ^{13}C NMR (100 MHz, $CDCl_3$, 298 K, relative to $SiMe_4$)/ppm: δ 165.06, 155.29, 153.46, 139.10, 128.37, 127.93, 60.66, 15.94. Positive FAB-MS: m/z 484 $[M]^+$. Anal. calc. for $C_{11}H_{10}BrN_2O_3Re{\cdot}\frac{1}{2}H_2O$: C, 26.78; H, 2.25; N, 5.68. Found: C, 26.84; H, 2.65; N, 5.76.

$[Ru(L1)(bpy)_2](PF_6)_2$ (4). This was synthesized using the modification of a literature procedure.[22] A mixture of $Ru(bpy)_2Cl_2$ (0.30 g, 0.63 mmol) and **L1** (0.32 g, 0.63 mmol) in absolute ethanol (45 ml) was heated to reflux under N_2 in the dark for 24 h. The reaction mixture was cooled to room temperature and concentrated to 5 ml, followed by filtration to give a dark red solution, to which a saturated NH_4PF_6 solution was added in a dropwise fashion until no further precipitation. Filtration followed by washing with ethanol and finally diethyl ether gave a red solid. Subsequent recrystallization by vapour diffusion of diethyl ether into an acetonitrile solution of the product gave **4** as dark red crystals. Yield: 0.32 g, 42%. ^{1}H NMR (400 MHz, CD_3CN, 298 K, relative to $SiMe_4$)/ppm: δ 10.32 (s, 1H, N═CH), 8.76 (s, 1H, ArH), 8.45–8.46 (m, 2H, ArH), 8.30–8.35 (m, 3H, ArH), 7.95–8.12 (m, 6H, ArH), 7.74–7.76 (m, 1H, ArH), 7.54–7.64 (m, 4H, ArH), 7.30–7.45 (m, 5H, ArH), 7.21 (s, 1H, ArH), 7.09 (d, J = 7.4 Hz, 1H, ArH), 6.77– 6.85 (m, 4H, ArH), 6.27 (s, 2H, NH), 3.52–3.54 (m, 4H, N–*CH_2*–CH_3), 2.07–2.10 (m, 6H, CH_3 on xanthene ring 1.36 (t, J = 7.1 Hz, 6H, N–CH_2–*CH_3*). ^{13}C NMR (100 MHz, $(CD_3)_2CO$, 298 K, relative to $SiMe_4$)/ppm: δ 170.17, 169.65, 164.35, 161.61, 158.20 158.08, 157.50, 157.10, 155.85, 154.80, 154.55, 153.40, 152.76, 152.74, 151.00, 150.33, 139.44, 139.11, 138.63, 138.44, 138.34, 137.72, 135.07, 135.05, 131.51, 130.11, 129.86, 128.67, 128.55, 127.41, 126.49, 126.46, 125.33, 124.97, 124.68, 124.49, 123.71, 123.68, 121.02, 119.06, 105.71, 105.65, 96.95, 96.88, 38.80, 38.67, 17.77, 17.34, 14.59, 14.50. Positive FAB-MS: m/z 466 $[M - 2PF_6]^{2+}$. Anal. calc. for $C_{52}H_{47}F_{12}N_9O_2P_2Ru{\cdot}\frac{1}{2}H_2O$: C, 50.78; H, 3.93; N, 10.25. Found: C, 50.82; H, 3.88; N, 10.01.

$[Ru(L2)(bpy)_2](PF_6)_2$ (5). This was prepared by a method similar to that of **4** except **L2** (0.34 g, 0.63 mmol) was used instead of **L1**. Complex **5** was isolated as orange crystals. Yield: 0.37 g, 48%. ^{1}H NMR (400 MHz, CD_3CN, 298 K, relative to $SiMe_4$)/ppm: δ 8.84 (s, 1H, N═CH), 8.39 (d, J = 6.2 Hz, 2H, ArH), 8.18 (d, J = 7.3 Hz, 1H, ArH), 8.12 (d, J = 7.5 Hz, 2H, ArH), 7.86–8.06 (m, 6H, ArH), 7.70–7.72 (m, 1H, ArH), 7.61 (d, J = 4.6 Hz, 1H, ArH), 7.49 (t, J = 6.2 Hz, 1H, ArH), 7.32–7.42 (m, 8H, ArH), 7.08 (t, J = 5.1 Hz, 1H, ArH), 6.78–6.80 (m, 1H, ArH), 6.45 (s, 1H, xanthene H), 6.25 (s, 1H, xanthene H), 6.07 (s, 1H, xanthene H), 5.91 (s, 1H, xanthene H), 4.27–4.28 (m, 1H, NCH_2CH_2N), 4.03–4.12 (m, 2H, NH), 3.23–3.48 (m, 5H, N–*CH_2*–CH_3 + NCH_2CH_2N), 2.55–2.60 (m, 1H, NCH_2CH_2N), 2.24–2.30 (m, 1H, NCH_2CH_2N), 1.80–1.82 (m, 6H, CH_3 on xanthene ring), 1.38 (t, J = 6.8 Hz, 3H, N–CH_2–*CH_3*); 1.31 (t, J = 6.7 Hz, 3H, N–CH_2–*CH_3*). ^{13}C NMR (100 MHz, $(CD_3)_2CO$, 298 K, relative to $SiMe_4$)/ppm: δ 170.62, 169.22, 157.79, 157.62, 157.49, 157.17, 155.28, 153.35, 153.19, 152.81, 152.40, 152.03, 151.91, 151.77, 149.01, 148.77, 139.20, 139.18, 139.09, 138.76, 138.55, 133.68, 130.51, 130.15, 129.35, 129.00, 128.79, 128.62, 128.11, 128.06, 127.93, 125.21, 125.14, 124.89, 124.82, 124.34, 123.29, 119.40, 119.38, 119.25, 106.08, 105.64, 97.58, 97.44, 65.57, 60.80, 41.48, 38.97, 38.89, 17.07, 17.00, 14.81, 14.75. Positive FAB-MS: m/z 480 $[M - 2PF_6]^{2+}$. Anal. calc. for $C_{54}H_{51}F_{12}N_9O_2P_2Ru$: C, 51.93; H, 4.12; N, 10.09. Found: C, 51.76; H, 4.42; N, 9.91.

$[Ru(L3)(bpy)_2](PF_6)_2$ (6). This was prepared by a method similar to that of **4** except **L3** (0.08 g, 0.63 mmol) was used instead of **L1**. Complex **6** was isolated as brownish-orange crystals. Yield: 0.24 g, 46%. ^{1}H NMR (400 MHz, CD_3CN, 298 K, relative to $SiMe_4$)/ppm: 8.94 (s, 1H, N═CH), 8.44–8.53 (m, 4H, ArH), 7.99–8.20 (m, 7H, ArH), 7.71 (s, 2H, ArH), 7.48–7.56 (m, 4H, ArH), 7.32–7.40 (m, 3H, ArH), 3.68 (q, J = 7.3 Hz, 1H, CH_2), 3.40 (q, J = 7.3 Hz, 1H, CH_2), δ 0.97 (t, J = 7.3 Hz, 3H, CH_3). ^{13}C NMR (100 MHz, $(CD_3)_2CO$, 298 K, relative to $SiMe_4$)/ppm: δ 167.96, 158.22, 158.11, 158.02, 157.89, 157.68, 153.63, 153.16, 152.82, 152.77, 152.03, 139.13, 139.10, 139.02, 138.91, 138.61, 130.17, 129.17, 129.03, 128.86, 128.77, 128.44, 125.22, 125.18, 125.05, 57.04, 14.71. Positive FAB-MS: m/z 274 $[M - 2PF_6]^{2+}$. Anal. calc. for $C_{28}H_{26}F_{12}N_6P_2Ru$: C, 40.15; H, 3.13; N, 10.03. Found: C, 40.52; H, 3.20; N, 9.92.

$[Ir(L1)(ppy)_2](PF_6)$ (7). This was synthesized using the modification of a literature procedure.[23] A mixture of $Ir_2(ppy)_4Cl_2$ (0.30 g, 0.28 mmol) and **L1** (0.29 g, 0.56 mmol) in a mixture of methanol/dichloromethane (1 : 1 v/v, 40 ml) was heated to reflux under N_2 in the dark for 4 h. The reaction mixture was then cooled to room temperature and a saturated NH_4PF_6 solution was added in a dropwise fashion until no further precipitation. Filtration followed by recrystallization by vapour diffusion of diethyl ether into a dichloromethane solution of the product gave **7** as dark red crystals. Yield: 0.38 g, 58%. ^{1}H NMR (400 MHz, $CDCl_3$, 298 K, relative to $SiMe_4$)/ppm: δ 8.67 (d, J = 4.9 Hz, 1H, ArH), 8.11–8.18 (m, 2H, ArH + N═CH), 7.64–7.83 (m, 6H, ArH), 7.59 (d, J = 4.4 Hz, 1H, ArH), 7.51 (d, J = 7.4 Hz, 1H, ArH), 7.40–7.47 (m, 2H, ArH), 7.31–7.37 (m, 2H, ArH), 7.01–7.06 (m, 2H, ArH), 6.72–6.89 (m, 6H, ArH), 6.49 (d, J = 6.4 Hz, 1H, ArH), 6.43 (s, 1H, ArH), 6.23 (s, 1H, xanthene H), 6.09 (s, 1H, xanthene H), 5.58 (s, 1H, xanthene H), 5.43 (d, J = 7.4 Hz, 1H, xanthene H), 3.87 (s, 1H, NH), 3.64 (s, 1H, NH), 3.15–3.36 (m, 4H, N–*CH_2*–CH_3), 1.97 (s, 3H, CH_3 on xanthene ring), 1.76 (s, 3H, CH_3 on xanthene ring), 1.35–1.41 (m, 6H, N–CH_2–*CH_3*). ^{13}C NMR (100 MHz, $(CD_3)_2CO$, 298 K relative to $SiMe_4$)/ppm: δ 169.30, 168.23, 167.35, 163.60, 153.98, 153.91, 153.78, 153.04, 152.03, 151.49, 150.01, 149.44, 149.29, 149.24, 147.60, 146.19, 144.86, 144.83, 140.49, 139.17, 138.58, 135.48, 134.76, 131.06, 131.02, 130.97, 130.80, 129.75, 129.24, 129.21, 129.11, 128.90, 125.20, 125.04, 124.11, 123.74, 123.60, 123.47, 122.40, 120.64, 120.46, 119.85, 119.39, 106.04, 104.98, 96.86, 96.64, 71.95, 38.80, 38.70, 30.42, 18.02, 17.35, 14.68, 14.57. Positive FAB-MS: m/z 1018 $[M - PF_6]^+$. Anal. calc. for $C_{54}H_{47}F_6IrN_7O_2P{\cdot}\frac{1}{4}CH_2Cl_2$: C, 55.01; H, 4.04; N, 8.28. Found: C, 55.01; H, 4.38; N, 8.28.

$[Ir(L2)(ppy)_2](PF_6)$ (8). This was prepared by a method similar to that of **7** except **L2** (0.30 g, 0.56 mmol) was used instead of **L1**. Complex **8** was isolated as orange crystals. Yield: 0.43 g, 65%. ^{1}H NMR (400 MHz, $CDCl_3$, 298 K, relative to

$SiMe_4$)/ppm: δ 8.29 (s, 1H, N=CH), 8.01–8.13 (m, 3H, ArH), 7.81–7.84 (m, 2H, ArH), 7.73–7.76 (m, 2H, ArH), 7.65–7.67 (m, 2H, ArH), 7.59 (d, J = 7.5 Hz, 1H, ArH), 7.42–7.44 (m, 3H, ArH), 7.33–7.38 (m, 2H, ArH), 7.15–7.17 (m, 1H, ArH), 6.75–7.04 (m, 6H, ArH), 6.39 (s, 1H, ArH), 6.22–6.28 (m, 2H, ArH), 6.02–6.08 (m, 3H ArH), 3.84–3.86 (m, 1H, NCH_2CH_2N), 3.58–3.61 (m, 2H, NH), 3.48–3.51 (m, 1H, NCH_2CH_2N), 3.13–3.36 (m, 5H, N–CH_2–CH_3 + NCH_2CH_2N), 2.30–2.35 (m, 1H, NCH_2CH_2N), 1.88–1.93 (m, 6H, CH_3 on xanthene rings), 1.33–1.40 (m, 6H, N–CH_2–CH_3). ^{13}C NMR (100 MHz, $(CD_3)_2CO$, 298 K, relative to $SiMe_4$)/ppm: δ 171.14, 168.96, 168.47, 168.34, 156.50, 155.31, 152.56, 152.21, 151.48, 151.22, 150.97, 150.30, 148.97, 148.84, 148.79, 148.66, 144.72, 144.21, 140.52, 139.42, 139.15, 133.52, 131.98, 131.94, 131.86, 131.09, 130.75, 130.68, 130.49, 128.92, 128.34, 127.99, 125.55, 125.34, 124.53, 124.46, 124.27, 123.53, 123.42, 123.20, 120.62, 120.33, 119.18, 119.12, 106.34, 105.70, 97.64, 97.50, 65.68, 60.33, 41.11, 38.96, 38.90, 17.15, 17.07, 14.83, 14.80. Positive FAB-MS: m/z 1046 $[M - PF_6]^+$. Anal. calc. for $C_{56}H_{51}F_6IrN_7O_2P$: C, 56.46; H, 4.32; N, 8.23. Found: 56.11; H, 4.26; N, 8.22.

$[Ir(L3)(ppy)_2](PF_6)$ (9). This was prepared by a method similar to that of 7 except Et-N-py (0.07 g, 0.56 mmol) was used instead of **L1**. Complex **9** was isolated as orange-yellow crystals. Yield: 0.30 g, 68%. ^{1}H NMR (400 MHz, $(CD_3)_2CO$, 298 K, relative to $SiMe_4$)/ppm: δ 9.57 (s, 1H, N=CH), 8.42–8.47 (m, 1H, ArH), 8.37 (dd, J = 0.72 and 5.8 Hz, 1H, ArH), 8.20–8.29 (m, 3H, ArH), 7.98–8.04 (m, 3H, ArH), 7.86 (dd, J = 1.6 and 6.1 Hz, 2H, ArH), 7.73–7.75 (m, 2H, ArH), 7.24–7.28 (m, 2H, ArH), 6.96–7.00 (m, 2H, ArH), 6.84–6.88 (m, 2H, ArH), 6.33 (d, J = 6.8 Hz, 1H, ArH), 6.22 (d, J = 7.6 Hz, 1H, ArH), 3.87 (q, J = 7.2 Hz, 1H, CH_2), 3.77 (q, J = 7.2 Hz, 1H, CH_2), 0.99 (t, J = 7.2 Hz, 3H, CH_3) ^{13}C NMR (100 MHz, $(CD_3)_2CO$, 298 K, relative to $SiMe_4$)/ppm: δ 169.50, 168.84, 168.54, 156.90, 151.53, 151.33, 151.26, 150.53, 150.30, 144.90, 144.84, 140.63, 139.56, 139.51, 132.56, 132.03, 131.17, 130.83, 130.52, 130.31, 125.64, 125.47, 124.54, 124.51, 123.43, 123.11, 120.72, 120.59, 56.41, 14.84. Positive FAB-MS: m/z 635 $[M - PF_6]^+$. Anal. calc. for $C_{30}H_{26}F_6IrN_4P$: C, 46.21; H, 3.36; N, 7.19. Found: C, 45.94; H, 3.63; N, 7.18.

$[Rh(L1)(ppy)_2](PF_6)$ (10). This was synthesized using the modification of a literature procedure.[24] A mixture of $Rh_2(ppy)_4Cl_2$ (0.30 g, 0.33 mmol) and **L1** (0.35 g, 0.67 mmol) in a mixture of methanol/dichloromethane (1 : 1 v/v, 40 ml) was heated to reflux under N_2 in the dark for 4 h. The reaction mixture was then cooled to room temperature, and a saturated NH_4PF_6 solution was added in a dropwise fashion until no further precipitation. Filtration followed by recrystallization by vapour diffusion of diethyl ether into a dichloromethane solution of the product gave **10** as red-orange crystals. Yield: 0.36 g, 51%. ^{1}H NMR (400 MHz, $CDCl_3$, 298 K, relative to $SiMe_4$)/ppm: δ 8.74 (d, J = 5.4 Hz, 1H, ArH); 8.12 (t, J = 7.7 Hz, 1H, ArH), 8.05 (s, 1H, N=CH), 7.58–7.84 (m, 8H, ArH), 7.40–7.45 (m, 3H, ArH), 7.29–7.35 (m, 1H, ArH), 7.08–7.14 (m, 1H, ArH), 6.76–6.98 (m, 7H, ArH), 6.52 (d, J = 7.4 Hz, 1H, ArH), 6.45 (s, 1H, ArH), 6.22 (s, 1H, ArH), 6.17 (s, 1H, ArH), 5.55–5.59 (m, 2H, ArH), 3.75 (s, 1H, NH), 3.66 (s, 1H, NH), 3.19–3.33 (m, 4H, N–CH_2–CH_3), 1.93 (s, 3H, CH_3 on xanthene ring), 1.70 (s, 3H, CH_3 on xanthene ring), 1.36 (t, J = 7.1 Hz, 6H, N–CH_2–CH_3). ^{13}C NMR (100 MHz, $(CD_3)_2CO$, 298 K, relative to $SiMe_4$)/ppm: δ 166.83, 165.63, 165.31, 164.58, 164.45, 164.42, 164.21, 163.47, 159.39, 153.39, 153.05, 153.02, 152.47, 151.00, 149.85, 149.42, 149.12, 144.65, 140.83, 139.33, 139.18, 136.38, 135.00, 132.40, 130.85, 130.83, 130.20, 129.70, 129.63, 128.86, 128.81, 128.71, 128.70, 125.31, 124.89, 124.32, 124.04, 123.72, 123.59, 123.50, 123.27, 120.71, 120.45, 120.17, 119.55, 105.98, 104.34, 96.90, 96.52, 70.33, 38.79, 38.71, 18.19, 17.28, 14.66, 14.56. Positive FAB-MS: m/z 928 $[M - PF_6]^+$. Anal. calc. for $C_{54}H_{47}F_6N_7O_2PRh{\cdot}H_2O$: C, 59.40; H, 4.52; N, 8.98. Found: C, 59.08; H, 4.41; N, 8.91.

$[Rh(L2)(ppy)_2](PF_6)$ (11). This was prepared by a method similar to that of **10** except **L2** (0.37 g, 0.67 mmol) was used instead of **L1**. Complex **11** was isolated as orange-yellow crystals. Yield: 0.47 g, 65%. ^{1}H NMR (400 MHz, $CDCl_3$, 298 K, relative to $SiMe_4$)/ppm: δ 8.11–8.15 (m, 2H, ArH), 7.93–7.95 (m, 2H. ArH), 7.82 (s, 3H, ArH + N=CH), 7.72–7.74 (m, 2H, ArH), 7.65 (t, J = 11 Hz, 2H, ArH), 7.35–7.47 (m, 4H, ArH), 7.17–7.21 (m, 1H, ArH), 7.08–7.10 (m, 1H, ArH), 6.94–7.03 (m, 3H, ArH), 6.82–6.90 (m, 2H, ArH), 6.39 (s, 1H, ArH), 6.26–6.31 (m, 2H, ArH), 6.05–6.11 (m, 2H, ArH), 6.02 (s, 1H, ArH), 3.85–3.90 (m, 1H, NCH_2CH_2N), 3.47–3.64 (m, 2H, NCH_2CH_2N), 3.22–3.33 (m, 6H, N–CH_2–CH_3 + NH), 2.32–2.36 (m, 1H, NCH_2CH_2N), 1.86–1.89 (m, 6H, CH_3 on xanthene ring), 1.33–1.41 (m, 6H, N–CH_2–CH_3). ^{13}C NMR (100 MHz, $(CD_3)_2CO$, 298 K, relative to $SiMe_4$)/ppm: δ 169.51, 168.92, 168.00, 167.68, 166.38, 166.06, 165.71, 165.57, 155.33, 154.57, 152.53, 152.22, 150.99, 150.89, 150.14, 148.81, 148.78, 148.64, 144.67, 144.20, 140.78, 139.55, 139.29, 133.49, 133.01, 132.95, 130.83, 130.70, 130.46, 130.23, 130.09, 128.90, 128.38, 128.04, 125.34, 125.14, 124.51, 124.43, 124.40, 124.30, 124.22, 123.19, 120.77, 120.55, 119.14, 119.09, 106.41, 105.74, 97.60, 97.48, 65.63, 59.36, 59.33, 41.09, 38.96, 38.90, 17.15, 17.08, 14.83, 14.79. Positive FAB-MS: m/z 957 $[M - PF_6]^+$. Anal. calc. for $C_{56}H_{51}F_6N_7O_2PRh{\cdot}\frac{1}{2}H_2O$: C, 60.54; H, 4.72; F, 10.26; N, 8.83. Found: C, 60.44; H, 4.70; N, 8.70.

$[Rh(L3)(ppy)_2](PF_6)$ (12). This was prepared by a method similar to that of **10** except Et-N-py (0.09 g, 0.67 mmol) was used instead of **L1**. Complex **12** was isolated as pale yellow crystals. Yield: 0.25 g, 68%. ^{1}H NMR (400 MHz, $(CD_3)_2CO$, 298 K, relative to $SiMe_4$)/ppm: δ 9.23 (s, 1H, N=CH), 8.29–8.38 (m, 4H, ArH), 8.23 (d, J = 9.1 Hz, 1H, ArH), 8.01–8.13 (m, 3H, ArH), 7.91 (d, J = 7.3 Hz, 2H, ArH), 7.73–7.75 (m, 2H, ArH), 7.30–7.34 (m, 2H, ArH), 7.04–7.07 (m, 2H, ArH), 6.90–6.96 (m, 2H, ArH), 6.34 (d, J = 7.8 Hz, 1H, ArH), 6.27 (d, J = 7.6 Hz, 1H, ArH), 3.69–3.76 (m, 2H, CH_2), 0.98 (t, J = 7.2 Hz, 3H, CH_3). ^{13}C NMR (100 MHz, $(CD_3)_2CO$, 298 K, relative to $SiMe_4$)/ppm: δ 168.21, 167.89, 167.80, 167.71, 167.39, 166.08, 166.06, 165.77, 165.75, 155.01, 151.05, 150.99, 150.39, 144.88, 144.78, 140.88, 139.70, 139.64, 133.53, 133.13, 130.90, 130.55, 130.04, 129.93, 125.42, 125.25, 124.54, 124.26, 124.03, 120.88, 120.87, 120.82, 120.80, 55.46, 14.81. Positive FAB-MS: m/z 562 $[M - PF_6]^+$. Anal. calc. for $C_{31}H_{30}F_6N_4PRh$: C, 52.70; H, 4.28; N, 7.93. Found: C, 52.14; H, 3.88; N, 8.16.

[Ir(L4)(terpy)](PF$_6$)$_3$ (13). This was synthesized by the modification of a literature procedure.[25] A mixture of Ir(terpy)Cl$_3$ (53 mg, 0.10 mmol) and **L4** (75 mg, 0.10 mmol) in degassed ethylene glycol (10 ml) was heated at 160 °C for 20 min under an inert atmosphere of nitrogen in the dark. The mixture was then cooled to room temperature and a saturated aqueous solution of NH_4PF_6 was added to precipitate an orange-red solid until no further precipitation occurred. The solid was washed with cold water and then a mixture of methanol and ether, and then dried under vacuum. Subsequent recrystallization of the complex from acetone–diethyl ether afforded **13** as air-stable orange-red crystals. Yield: 62 mg (52%).^{1}H NMR (400 MHz, CD_3OD, 298 K, relative to $SiMe_4$) δ 9.15 (s, 1H, ArH), 8.93 (d, J = 8.3 Hz, 2H, ArH), 8.75 (d, J = 8.0 Hz, 2H, ArH), 8.74–8.63 (m, 3H, ArH), 8.13 (m, 4H, ArH), 8.01–7.93 (m, 2H, ArH), 7.89–7.82 (m, 1H, ArH), 7.74–7.60 (m, 4H, ArH), 7.54–7.36 (m, 5H, ArH), 7.21–7.14 (m, 2H, ArH), 6.51 (d, J = 9.0 Hz, 2H, ArH), 6.29 (dd, J = 8.9, 2.6 Hz, 2H, ArH), 6.18 (d, J = 2.6 Hz, 2H, ArH), 3.22 (q, J = 7.0 Hz, 8H, CH_2), 1.00 (t, J = 7.0 Hz, 12H, CH_3). ^{13}C NMR (100 MHz, $(CD_3)_2CO$, 298 K, relative to $SiMe_4$)/ppm: δ 168.54, 159.44, 155.95, 155.77, 155.71, 155.20, 154.46, 154.20, 153.56, 149.91, 144.75, 143.78, 143.63, 142.58, 134.56, 132.12, 130.71, 130.66, 130.13, 129.35, 129.25, 129.22, 128.29, 127.68, 125.80, 124.65, 124.32, 123.97, 109.26, 107.14, 98.44, 67.86, 44.85, 12.89. Positive FAB-MS: m/z 1464 $[M - PF_6]^+$, 1319 $[M - 2PF_6]^+$, 1174 $[M - 3PF_6]^+$. Anal. calc. for $C_{64}H_{55}F_{18}IrN_9O_2P_3{\cdot}H_2O$: C, 47.24; H, 3.53; N, 7.75. Found: C, 47.20; H, 3.74; N, 7.69.

[Ru(L4)(terpy)](PF$_6$)$_2$ (14). This was synthesized using the modification of a literature procedure.[26] A mixture of Ru(tpy)Cl$_3$ (0.11 g, 0.25 mmol) and **L4** (0.19 g, 0.25 mmol) in absolute ethanol (25 ml) with a few drops of triethylamine was heated to reflux under N_2 in the dark for 24 h. The reaction mixture was cooled to room temperature and concentrated to about 5 ml, followed by filtration to give a red solution, and a saturated NH_4PF_6 solution was added in a dropwise fashion until no further precipitation occurred. Filtration followed by recrystallization by vapour diffusion of diethyl ether into an acetonitrile solution of the product gave **14** as red crystals. Yield: 0.18 g, 52%. ^{1}H NMR (400 MHz, CD_3CN, 298 K, relative to $SiMe_4$)/ppm: δ 8.90 (s, 2H, ArH), 8.73 (d, J = 8.2 Hz, 2H, ArH), 8.56 (d, J = 8.2 Hz, 2H, ArH), 8.47 (d, J = 7.4 Hz, 2H, ArH), 8.38–8.40 (m, 1H, ArH), 8.01–8.03 (m, 3H, ArH), 7.90 (t, J = 7.74 Hz, 4H, ArH), 7.57–7.65 (m, 2H, ArH), 7.41 (d, J = 8.7 Hz, 2H, ArH), 7.35 (d, J = 5.6 Hz, 2H, ArH), 7.31 (d, J = 4.8 Hz, 2H, ArH), 7.11–7.14 (m, 5H, ArH), 6.75 (d, J = 9.0 Hz, 2H, ArH), 6.44 (dd, J = 2.4 and 9.0 Hz, 2H, ArH), 6.38 (d, J = 2.3 Hz, 2H, ArH), 3.37 (q, J = 7.0 Hz, 8H, N–CH_2–CH_3), 1.14 (t, J = 7.1 Hz, 12H, N–CH_2–CH_3). ^{13}C NMR (100 MHz, $(CD_3)_2CO$, 298 K, relative to $SiMe_4$)/ppm: δ 168.41, 159.39, 159.24, 156.55, 156.43, 155.19, 153.68, 153.49, 153.38, 149.89, 148.23, 139.12, 139.04, 136.99, 134.40, 130.52, 129.41, 129.32, 128.60, 128.38, 126.42, 125.60, 125.43, 124.82, 124.70, 123.91, 121.84, 109.25, 107.29, 98.47, 67.81, 44.87, 12.91. Positive ESI-MS: m/z 542 $[M - 2PF_6]^{2+}$. Anal. calc. for $C_{64}H_{55}F_{12}N_9O_2P_2Ru{\cdot}3H_2O$: C, 53.86; H, 4.31; N, 8.83. Found: C, 53.60; H, 4.04; N, 8.72.

Physical measurements and instrumentation

All ^{1}H and ^{13}C NMR spectra were obtained using a Bruker AVANCE DPX 300 (300 MHz) or Bruker AVANCE DPX 400 (400 MHz) Fourier-transform NMR spectrometer with chemical shifts reported relative to tetramethylsilane, $(CH_3)_4Si$. Fast atom bombardment (FAB) and electron impact (EI) ionization mass spectra were obtained using a Finnigan MAT95 mass spectrometer. All positive-ion electrospray ionization (ESI) mass spectra were obtained using a Finnigan LCQ mass spectrometer. Elemental analyses of the compounds were carried out on a Carlo Erba 1106 elemental analyzer at the Institute of Chemistry of the Chinese Academy of Sciences, Beijing, China. The UV-visible absorption spectra were obtained using a Hewlett-Packard 8452A diode. Steady state emission spectra at room temperature were recorded on a Spex Fluorolog-3 Model FL3-211 fluorescence spectrofluorometer equipped with a R2658P PMT detector. Luminescence quantum yields for solution samples were measured on a Hamamatsu C11347-11 Absolute PL Quantum Yield measurement system.

Ion-binding studies

The electronic absorption and emission spectra of the titration experiments for determining the binding constant were measured on a Hewlett-Packard 8452A diode array spectrophotometer and on a Spex Fluorolog-3 Model FL3-211 fluorescence spectrofluorometer, respectively. Binding constants for the 1 : 1 complexation were determined by nonlinear least-squares fits to eqn (1):

$$X = X_0 + \frac{X_{\lim} - X_0}{2[\mathrm{M}]_\mathrm{T}}\{[\mathrm{M}]_\mathrm{T} + [\mathrm{G}] + 1/K_\mathrm{S} - [([\mathrm{M}]_\mathrm{T} + [\mathrm{G}] + 1/K_\mathrm{S})^2 - 4[\mathrm{M}]_\mathrm{T}[\mathrm{G}]]^{1/2}\} \quad (1)$$

in which the derivations were previously described as follows:[27] X_0 and X are the absorbance (or luminescence intensity) of the host complexes at a selected wavelength in the absence and presence of Hg(II) ions, respectively, $[M]_T$ is the total concentration of the host complexes, [G] is the concentration of the guest, *e.g.* metal ion, X_{lim} is the limiting value of absorbance (or luminescence intensity) in the presence of excess guest, and K_s is the stability constant.

X-Ray crystal structure determination†

All the experimental details are given in Table 1. Single crystals of **11** suitable for X-ray diffraction studies were grown by slow diffusion of diethyl ether vapor into a dichloromethane solution of the complex. A crystal of the dimensions 0.3 × 0.25 × 0.2 mm mounted in a glass capillary was used for data collection on a Bruker Smart CCD 1000 using graphite monochromatized Mo-K$_\alpha$ radiation (λ = 0.71073 Å) at 28 °C. The structure was solved by direct methods employing the SHELXS-97 program.[28] Rh and many non-H atoms were located according to the direct methods. The positions of the other non-hydrogen atoms were found after successful refinement by full-matrix least-squares using the program SHELXL-97.[29] There

Table 1 Crystal and structure determination data of **11**

	11
Empirical formula	$C_{56}H_{49}F_6N_7O_2PRh$
Formula weight	1099.90
Temperature (K)	298(2)
Wavelength (Å)	0.71073
Crystal system	Trigonal
Space group	$R\bar{3}$
a (Å)	23.030(5)
b (Å)	23.030(5)
c (Å)	64.884(12)
α (°)	90
β (°)	90
γ (°)	120
Volume (Å^3)	29 802(13)
Z	18
Density (calculated) (g cm^{-3})	1.103
Crystal size, mm × mm × mm	0.12 × 0.21 × 0.22
Index ranges	$-29 \le h \le 25$ $-29 \le k \le 29$ $-75 \le l \le 67$
Reflections collected/unique	36 615/13 553 [R(int) = 0.0816]
Completeness (%)	91.2 (two theta = 25.242°)
Data/restraints/parameters	13 553/2/647
Goodness-of-fit on F^2	0.899
Final R indices[a] [$I > 2\sigma(I)$]	R_1 = 0.0653 wR_2 = 0.1782
Largest difference peak and hole (e Å^{-3})	0.493 and −0.652

[a] $R_{int} = \sum|F_o^2 - F_o^2\,(mean)|/\sum[F_o^2]$, $R_1 = \sum||F_o| - |F_c||/\sum|F_o|$, and $wR_2 = \{\sum[w(F_o^2 - F_c^2)^2]/\sum[w(F_o^2)^2]\}^{1/2}$.

was one formula unit in the asymmetric unit. Two one thirds of PF_6 were located in two positions, but the other one third of PF_6 could not be located. Full-matrix least-squares refinement on F^2 was used in the structure refinement. The positions of the H atoms were calculated based on the riding mode with the thermal parameters equal to 1.2 times those of the associated C atoms, and participated in the calculation of the final R-indices. One crystallographic asymmetric unit consists of one formula unit. In the final stage of least-squares refinement, all non-hydrogen atoms were refined anisotropically.

Results and discussion

Synthesis and characterization

The ligands **L1** and **L2** were synthesized from the intermediates, rhodamine 6G hydrazide and rhodamine 6G ethylamine, respectively, which were prepared by the reaction of rhodamine 6G and hydrazine monohydrate or ethane-1,2-diamine in absolute ethanol at reflux under N_2 for 24 h (Scheme 2). Rhodamine hydrazide and rhodamine 6G ethylamine were then subjected to a condensation reaction with 2-pyridinecarboxaldehyde in methanol at reflux under N_2 for 3 h, followed by recrystallization from dichloromethane–diethyl ether or only filtration to afford **L1** and **L2** in a reasonable yield. The analogue ligand without the rhodamine moiety, **L3**, was synthesized through addition of ethylamine to 2-pyridinecarboxaldehyde under stirring in an ice-water bath for 2 h and at room temperature for another 2 h, followed by extraction with diethyl ether to afford the ligand in a high yield. The synthetic methodology of ligand **L4** is depicted in Scheme 2, in which the rhodamine B base and 4′-(4-amino-phenyl)-2,2′:6′,2″-terpyridine were reacted in the presence of $POCl_3$ and Et_3N in dry 1,2-dichloroethane to give **L4**. **L1–L4** were characterized by ^{1}H NMR spectroscopy and FAB or EI mass spectrometry. The complexes were synthesized through incorporation of these rhodamine-containing (**L1**, **L2** and **L4**) or rhodamine-free (**L3**) ligands into various transition metal precursors including $Re(CO)_5Br$, $Ru(bpy)_2Cl_2$, $Ir_2(ppy)_4Cl_2$, $Ir(terpy)Cl_3$ and $Ru(terpy)Cl_3$. The identities of complexes **1–14** were confirmed by ^{1}H NMR spectroscopy, satisfactory elemental analyses and positive-ion FAB or ESI mass spectrometric methods.

X-ray crystal structure

Single crystals of **11** were obtained by slow diffusion of diethyl ether vapor into a dichloromethane solution of the complex, and the structure was solved by X-ray crystallography. The perspective drawing is shown in Fig. 1 and the selected bond distances (Å) and angles (°) are given in Table 2. The structure of **11** shows a distorted octahedral geometry about the rhodium(III)

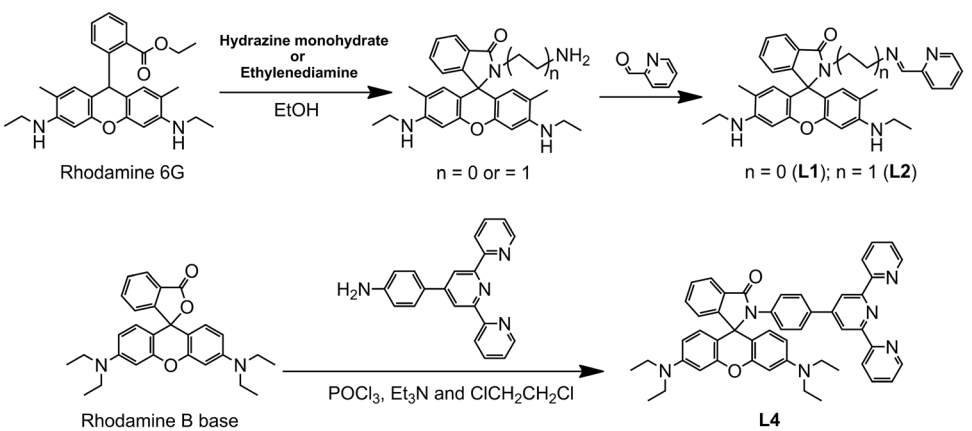

Scheme 2 Synthetic pathways of **L1**, **L2** and **L4**.

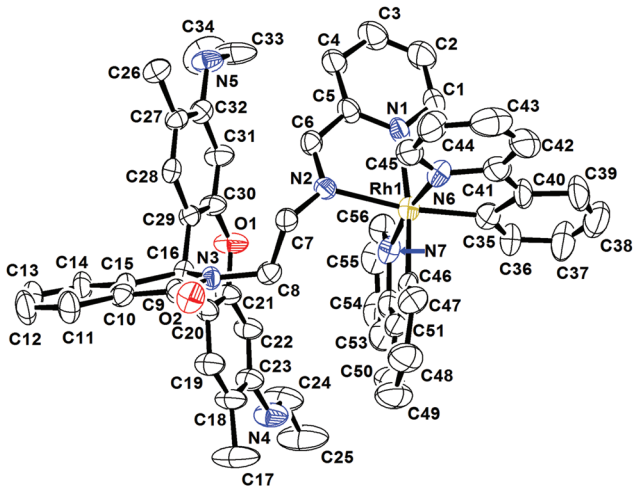

Fig. 1 Perspective drawing of the complex cation of **11** with atomic numbering scheme. Hydrogen atoms are omitted for clarity. Thermal ellipsoids are drawn at the 25% probability level.

Table 2 Selected bond lengths (Å) and angles (°) for **11** with estimated standard deviations (esds) given in parentheses

Bond lengths (Å)	
Rh(1)–N(1)	2.166(5)
Rh(1)–N(2)	2.161(5)
Rh(1)–N(6)	2.014(6)
Rh(1)–N(7)	2.020(6)
Rh(1)–C(35)	1.988(8)
Rh(1)–C(46)	1.977(6)
C(15)–C(16)	1.530(8)
N(3)–C(16)	1.478(6)
C(16)–C(20)	1.503(7)
C(16)–C(29)	1.509(7)
Bond angles (°)	
N(1)–Rh(1)–N(2)	76.60(19)
N(6)–Rh(1)–C(35)	80.4(3)
N(7)–Rh(1)–C(46)	80.9(3)
C(8)–N(3)–C(9)	123.0(5)
C(8)–N(3)–C(16)	122.7(4)
C(9)–N(3)–C(16)	114.2(5)

metal centre, which was commonly observed in other related cyclometallated rhodium(III) complexes.[24] Each of the nitrogen atoms of the diimine ligand of **L2** is in *trans* position to the carbon atoms of the cyclometallating C^N ligands (HC^N = 2-phenylpyridine). The N–Rh–N and N–Rh–C bond angles from 76.6–80.9° deviated from the idealized value of 90°, due to the bite distances exerted by the steric requirements of the chelating cyclometallating and diimine ligands. Other bond angles and bond distances about the rhodium(III) metal centre are similar to those found in other related cyclometallated rhodium(III) complexes.[24] The molecular structure clearly shows that the rhodamine derivative is in a ring-closed form with the spirolactam ring at the spiro carbon C(16), with a C(15)–C(16)–N(3) bond angle of 100.7° and a N(3)–C(16) bond distance of 1.478 Å. The plane of 2-amino-2,3-dihydro-1*H*-isoindol-1-one and that of xanthene are essentially orthogonal to each other with a dihedral angle of 88.69°.

Electronic absorption and emission properties

The photophysical properties of all complexes **1–14** were studied in acetonitrile at 298 K and their photophysical data are given in Table 3. By scrutinizing the electronic absorption data of complexes **1–12** with the same metal centres (**1–3** for Re^{I}, **4–6** for Ru^{II}, **7–9** for Ir^{III} and **10–12** for Rh^{III}) and with the same ligands (**1**, **4**, **7** and **10** for **L1**; **2**, **5**, **8** and **11** for **L2**; **3**, **6**, **9** and **12** for **L3**), the intense high-energy absorption bands at *ca.* 262–306 nm with extinction coefficients of the order of 10^4 $dm^3\ mol^{-1}\ cm^{-1}$ are attributed to the spin-allowed intraligand (^{1}IL) [$\pi \rightarrow \pi^*$] transitions of the diimine moiety and rhodamine derivative (with the exception of **L3**). The electronic absorption spectra of complexes **1–3** (as depicted in Fig. 2) show extra low-energy absorption bands at *ca.* 402–430 nm. The low-energy absorption bands are assigned to the spin-allowed metal-to-ligand charge transfer (MLCT) [dπ(Re) $\rightarrow$ π^*(diimine)] transitions.[21] The observation of a red-shift of the MLCT absorption band in **1** (430 nm), relative to those in **2** (406 nm) and **3** (402 nm), is ascribed to the lower π^*(diimine) energy level as a result of the higher conjugation from the Schiff base diimine chelating ligand to the rhodamine derivative. Fig. 3 shows representative electronic absorption spectra of **5**, **8** and **11**. For the ruthenium(II) diimine complexes **4–6** (Fig. S1†), broad low-energy absorption bands at 420–468 nm were observed, assignable to the spin-allowed metal-to-ligand charge transfer (MLCT) [dπ(Ru) $\rightarrow$ π^*(diimine)] transitions. A characteristic

Table 3 Electronic absorption and emission data of complexes **1–14** in acetonitrile at 298 K

Complex	Absorption λ/nm (ε/$dm^3\ mol^{-1}\ cm^{-1}$)	Emission (Φ_{lum})
1	262 sh (38 460), 304 (23 145), 334 (12 455), 350 (11 470), 430 (4340)	692 ($<10^{-4}$)
2	262 sh (37 450), 300 (19 500), 406 (3580)	672 ($<10^{-4}$)
3	270 (10 660), 402 (3625)	663 ($<10^{-4}$)
4	285 (62 030), 349 sh (12 110), 424 (9565), 490 sh (17 725),[a] 529 (35 760)[a]	551[a] (—[c])
5	286 (70 190), 343 (7365), 421 (10 650), 468 (14 350)	720 ($<10^{-4}$)
6	287 (30 465), 420 sh (5770), 464 (7830)	698 ($<10^{-4}$)
7	263 sh (65 565), 300 (34 965), 407 (6520), 520 sh (1150)	546[a] (—[c])
8	262 sh (63 740), 298 (29 450), 380 (8155), 520 sh (605)	660 ($<10^{-4}$)
9	266 sh (45 480), 300 (9865), 370 (8765), 522 sh (460)	645 (0.17)
10	262 sh (64 960), 301 (52 520), 362 (9850)	548[a] (—[c])
11	264 sh (56 610), 298 (30 505), 370 (7440)	558 ($<10^{-4}$)
12	263 (41 580), 306 sh (18 885), 372 (7280)	552 (0.05)
13	273 (70 950), 310 (82 695), 328 sh (55 920), 485 (24 935), 564 sh (3115)	—[b]
14	280 (66 230), 312 (46 670), 354 (23 425), 374 (20 635)	—[b]

[a] Characteristic of rhodamine 6G absorption or emission due to the occurrence of ring opening. [b] Non-emissive. [c] Not determined.

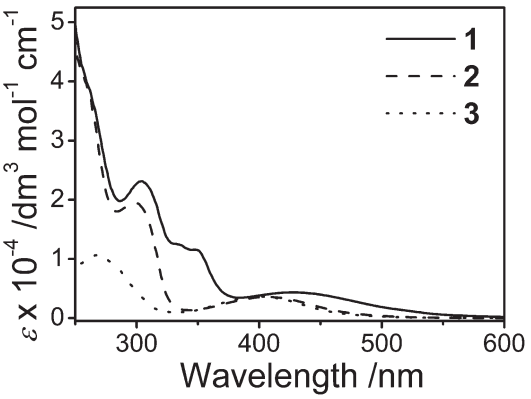

Fig. 2 Electronic absorption spectra of **1–3** in acetonitrile at 298 K.

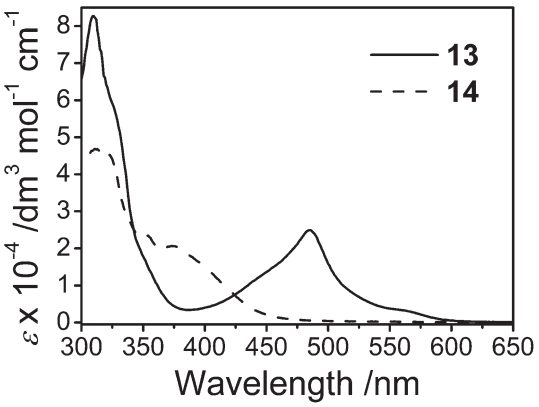

Fig. 4 Electronic absorption spectra of **13** and **14** in acetonitrile at 298 K.

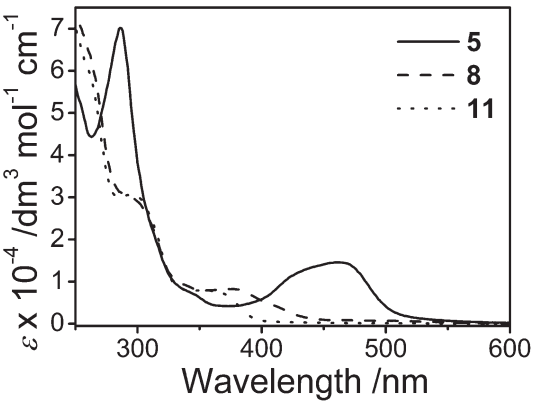

Fig. 3 Electronic absorption spectra of **5**, **8** and **11** in acetonitrile at 298 K.

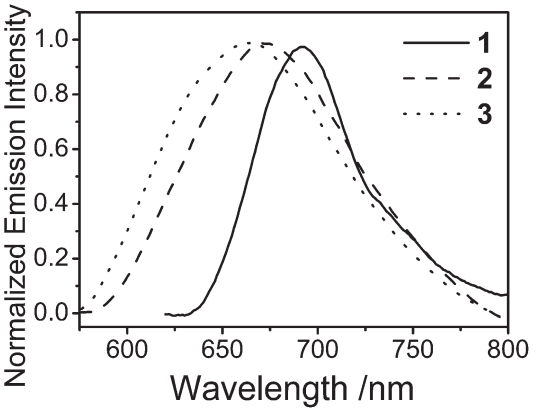

Fig. 5 Normalized emission spectra of **1–3** in acetonitrile at 298 K.

rhodamine 6G absorption band was also observed in **4**, probably due to the occurrence of ring opening of the rhodamine derivative in acetonitrile. The electronic absorption properties of **7–12** are illustrated in Fig. S2 and S3.† Low-energy absorption bands were observed at 370–407 nm for the cyclometallated iridium(III) diimine complexes **7–9**, while the rhodium(III) congeners **10–12** showed low-energy absorption bands at 362–372 nm. According to the spectroscopic studies on the related cyclometallated iridium(III)[23,30] and rhodium(III)[24] systems, such low-energy absorption bands involve spin-allowed metal-to-ligand charge transfer (^{1}MLCT) [dπ(Ir or Rh) → π*(diimine and cyclometallating ligands)] transitions. An additional weak shoulder occurring beyond 520 nm for **7–9** is tentatively assigned to a spin-forbidden ^{3}MLCT transition, resulting from the spin–orbit coupling of an iridium(III) heavy atom. For ruthenium(II) and iridium(III) terpyridyl complexes **13** and **14**, their electronic absorption spectra are depicted in Fig. 4. Intense high-energy absorption bands at 273–329 nm and intense low-energy absorption bands at 485–564 nm were observed for **13**, while intense high-energy absorption bands at 280–354 nm and a low-energy absorption shoulder at *ca.* 374 nm were observed for **14**. These low-energy absorption bands are assigned to the metal-to-ligand charge transfer (MLCT) [dπ(Ir or Ru) → π*(terpyridine)] transitions.[25,26]

The emission behaviours of complexes **1–14** in acetonitrile at room temperature were investigated and the results are summarized in Table 3. Depending on the nature of the transition metal centres, chelating ligands as well as the linker to the rhodamine derivative, they exhibited various emission properties with λ_{em} in the range of 546–720 nm upon excitation at λ > 320 nm. The emission spectra of the rhenium(I) tricarbonyl diimine complexes **1**, **2** and **3** are illustrated in Fig. 5. Emission with λ_{em} at 663–692 nm was observed, which is suggested to originate from the triplet metal-to-ligand charge transfer (^{3}MLCT) [dπ(Re) → π*(N^N)] excited state.[21] In general, this class of complexes exhibited lower emission energies than those of the related rhenium(I) tricarbonyl bipyridine system, in view of the lower π* energy level of the Schiff base diimine chelating ligand. Similar to the electronic absorption results, the emission energy of **1** (692 nm) was lower than those of complex **2** (672 nm) and **3** (663 nm), which can be ascribed to the lower-lying π* orbital in **1** as a result of the higher degree

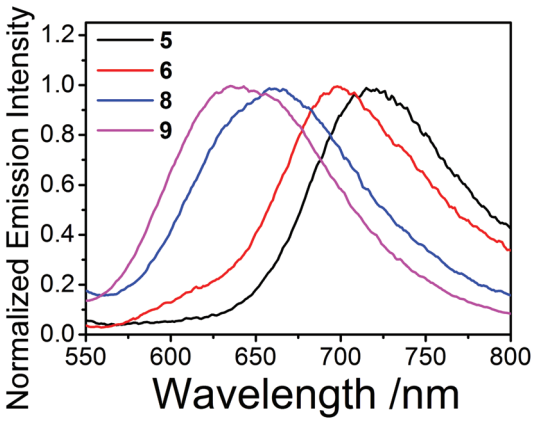

Fig. 6 Normalized emission spectra of **5**, **6**, **8** and **9** in acetonitrile at 298 K.

of π-conjugation between the rhodamine moiety and the pyridine-imine moiety. The ruthenium(II) diimine complexes (**5** and **6**) and the cyclometallated iridium(III) diimine complexes **8** and **9** were found to exhibit emissions at 698–720 nm and 645–660 nm, respectively (Fig. 6). These emissions are attributed to the existence of a triplet metal-to-ligand charge transfer (^{3}MLCT) [dπ(Ru or Ir) → π*(N^N)] character.[23,30,31] On the other hand, characteristic bands of the rhodamine 6G emission at 546–551 nm were observed in **4** and **7** due to the presence of the ring-opened form of the rhodamine moiety with a much higher emission quantum yield, relative to that of the ruthenium(II) and cyclometallated iridium(III) diimine systems. The cyclometallated rhodium(III) diimine system displayed emission at 544–558 nm, which is suggested to be derived from the triplet excited state of intraligand (^{3}IL) [π → π*(N^C)] transition, mixed with the metal-to-ligand charge transfer (^{3}MLCT) [dπ(Rh) → π*(N^C)] character.[24] It is interesting to note that the luminescence quantum yields for the rhodamine-tethered iridium(III) complexes, **7** and **8**, and the rhodium(III) complexes, **10** and **11**, are lower than those of the corresponding rhodamine free complexes, **9** and **12**. This is probably due to the efficient nonradiative decay resulting from the fluxional behaviour of the bulky rhodamine substituent. The emission spectrum of **12**, which contains no rhodamine derivative, is shown in Fig. S5.† Mixing with the rhodamine 6G emission, which shows emission at a similar energy, could be possible in **10** and **11**. The iridium(III) and ruthenium(II) terpyridyl complexes **13** and **14** were found to be non-emissive or weakly emissive.

Cation-binding studies

The binding properties of the complexes tethered with rhodamine derivatives (**1**, **2**, **4**, **5**, **7**, **8**, **10**, **11**, **13** and **14**) were investigated by electronic absorption and emission spectroscopic methods for various alkali, alkaline-earth and transition-metal cations such as K^+, Na^+, Li^+, Ca^{2+}, Mg^{2+}, Ba^{2+}, Pb^{2+}, Cd^{2+}, Zn^{2+}, Co^{2+}, Ni^{2+}, Ag^+, Fe^{2+}, Cu^{2+} and Hg^{2+}. No remarkable colour change or new electronic absorption band could be found upon addition of such cations to the acetonitrile solutions of **2**, **5**, **8** and **11** (containing **L2**) as well as **13** and **14** (containing **L3**), suggesting that no observable ring opening process from the rhodamine derivative occurred. This is probably due to the remote connection of the rhodamine derivatives to the transition metal moieties, with an ethylene or phenyl group spacer. On the other hand, complexes **1**, **4**, **7** and **10** containing **L1** with the rhodamine derivative directly linked to the imine nitrogen, were found to exhibit remarkable spectral changes in the presence of certain metal cations. The incorporation of the transition metal moiety, which is in close proximity to the rhodamine derivative, may lead to a higher tendency toward the ring-opening process.

Addition of Hg^{2+}, Ag^+, Pb^{2+}, Cu^{2+} and Zn^{2+} ions to the solution of rhenium(I) tricarbonyl diimine complex **1** was found to give a new absorption band at about 530 nm in the electronic absorption spectra, concomitant with the solution colour change to magenta. On the basis of the absorption band of rhodamine 6G occurring at a similar energy, the emergence of this absorption band is ascribed to the conversion of the spirolactam form to the corresponding ring-opened amide form.[4] Well-defined isosbestic points were observed, indicative of a clean conversion in equilibrium. The corresponding electronic absorption spectral changes upon addition of Hg^{2+}, Ag^+, Pb^{2+}, Cu^{2+} and Zn^{2+} are depicted in Fig. 7 and 8, and Fig. S6–8,† respectively, together with the plots of absorbance at 530 nm against the concentration of cations (shown in the insets). From the results of the theoretical fit of the 1 : 1 stoichiometric binding mode with experimental data, the binding constants (log K_s values) for Hg^{2+}, Ag^+ and Pb^{2+} ion binding were determined to be 7.17, 4.88 and 5.85, respectively (Table 4). Ruthenium(II) diimine complex **4** was found to show the rhodamine

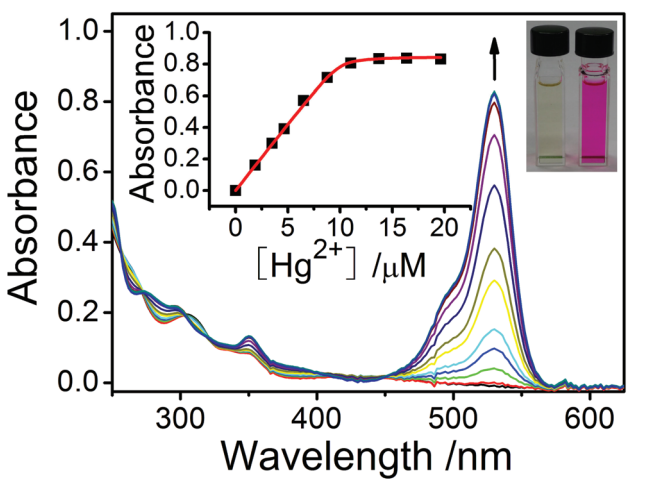

Fig. 7 Electronic absorption spectral changes of **1** in CH_3CN (concentration = 9.66 μM) at 298 K upon addition of various concentrations of Hg^{2+}. Insets show the photograph of color changes and the plot of the absorbance at 530 nm as a function of the concentration of Hg^{2+} with a theoretical fit.

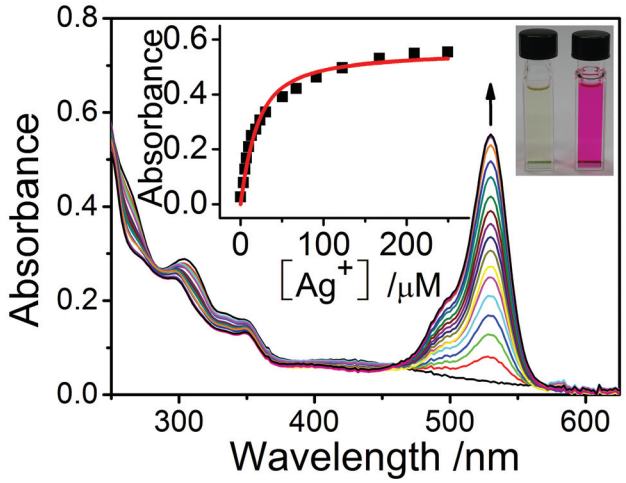

Fig. 8 Electronic absorption spectral changes of **1** in CH_3CN (concentration = 11.8 μM) at 298 K upon addition of various concentrations of Ag^+. Insets show the photograph of color changes and the plot of the absorbance at 530 nm as a function of the concentration of Ag^+ with a theoretical fit.

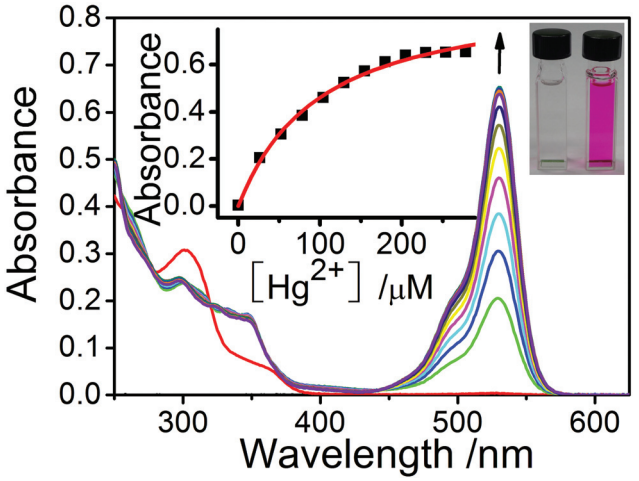

Fig. 9 Electronic absorption spectral changes of **10** in CH_3CN (11.8 μM) at 298 K upon addition of various concentrations of Hg^{2+}. Insets show the photograph of color changes and the plot of the absorbance at 530 nm as a function of the concentration of Hg^{2+} with a theoretical fit.

Table 4 Binding constants of complexes **1** and **7** with various cations in acetonitrile

Complexes	M^+	Log K_s
1	Hg^{2+}	7.17 ± 0.01^a
	Ag^+	4.88 ± 0.06^a
		4.34 ± 0.02^b
	Pb^{2+}	5.85 ± 0.25^a
7	Hg^{2+}	4.04 ± 0.04^b
		4.81 ± 0.08^b

[a] From electronic absorption titration studies. [b] From emission titration studies.

6G absorption at 530 nm upon addition of Hg^{2+}, Pb^{2+}, Cu^{2+} and Zn^{2+} (Fig. S8–S11†), while the cyclometallated iridium(III) diimine complex **7** showed similar spectral response with Hg^{2+}, Pb^{2+} and Cu^{2+} (Fig. S12–S14†). It is noteworthy that the cyclometallated rhodium(III) diimine complex **10** exhibited selective sensing behaviour. Only Hg^{2+} was able to induce the ring opening of the rhodamine derivative with the emerging absorption band at 530 nm. Fig. 9 shows the electronic absorption spectral changes of **10** with varying Hg^{2+} concentration. The log K_s value of 4.04 for Hg^{2+} ion binding was estimated from the satisfactory result of the theoretical fit of the 1 : 1 stoichiometric binding mode. Table 5 summarizes the sensing responses towards various metal cations. In general, the complexes would give two reporting states of "ON" or "OFF". The

Table 5 Sensing responses of complexes **1**, **4**, **7** and **10** towards various cations in acetonitrile at 298 K[c]

		1	**4**	**7**	**10**
Hg^{2+}	State	"ON"	"ON"	"ON"	"ON"
	Detection limit	2×10^{-6} M[a]	1×10^{-6} M[a]	4×10^{-7} M[a]	4×10^{-7} M[b]
		4×10^{-7} M[b]		4×10^{-7} M[b]	
Pb^{2+}	State	"ON"	"ON"	"ON"	"OFF"
	Detection limit	9×10^{-7} M[a]	7×10^{-7} M[a]	1×10^{-6} M[a]	
		4×10^{-7} M[b]		4×10^{-7} M[b]	
Cu^{2+}	State	"ON"	"ON"	"ON"	"OFF"
	Detection limit	7×10^{-7} M[a]	6×10^{-7} M[a]	5×10^{-7} M[a]	
		4×10^{-7} M[b]	2×10^{-7} M[b]	3×10^{-7} M[b]	
Zn^{2+}	State	"ON"	"ON"	"OFF"	"OFF"
	Detection limit	1×10^{-6} M[a]	3×10^{-7} M[a]		
Ag^+	State	"ON"	"OFF"	"OFF"	"OFF"
	Detection limit	2×10^{-6} M[a]			
		3×10^{-6} M[b]			

[a] From electronic absorption titration studies. [b] From emission titration studies. [c] Reporting state "ON" represents that the complex exhibits a positive sensing response, while the state "OFF" represents that the complex exhibits no observable or a negligible sensing response towards a certain cation.

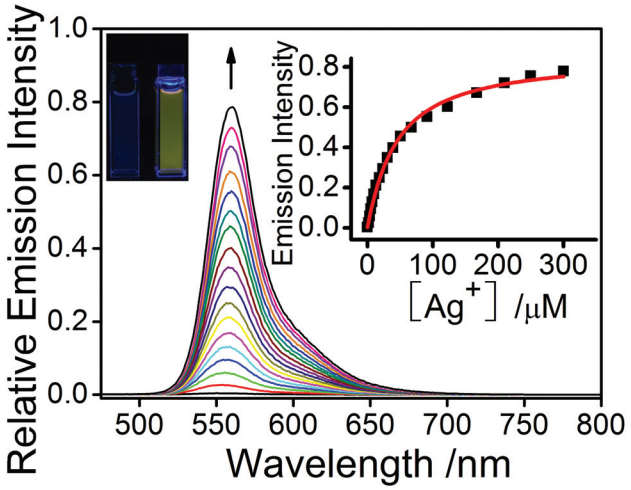

Fig. 10 Emission spectral changes of **1** (11.8 μM) in acetonitrile at 298 K upon addition of various concentrations of Ag^{+}. Insets show the photograph of emission enhancement and the plots of the emission intensity at 560 nm as a function of the concentration of Ag^{+} with a theoretical fit.

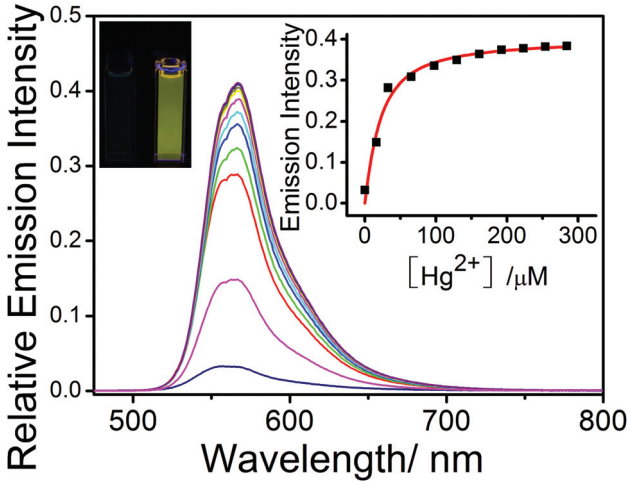

Fig. 11 Emission spectral changes of **10** (11.8 μM) in acetonitrile at 298 K upon addition of various concentrations of Hg^{2+}. Insets show the photograph of emission enhancement and the plots of the emission intensity at 560 nm as a function of the concentration of Hg^{2+} with a theoretical fit.

"ON" state from the complexes represents the positive sensing response for a certain cation with emergence of a new absorption band at about 530 nm and an intense emission at 560 nm. The reporting state "OFF" of the complexes represents no observable or a negligible sensing response for a certain cation. Detection limits in the range of 10^{-6}–10^{-7} M were estimated for **1**, **4**, **7** and **10** from the electronic absorption titration results. Although no rational relationship could be concluded, different selectivities, sensitivities as well as binding stabilities of **1**, **4**, **7** and **10** have proven that the nature of the transition metal centres, even with the same **L1** ligand, plays an important role in the sensing properties of the rhodamine derivative.

Emission titration studies were also performed to examine the ion binding abilities of **1**, **4**, **7** and **10**. In general, their emission spectral responses towards various metal cations were consistent with the electronic absorption results. Upon excitation at the isosbestic points found in the electronic absorption titration, an intense emission at 560 nm was observed for **1** with increasing concentrations of Hg^{2+}, Ag^{+}, Pb^{2+}, Cu^{2+} and Zn^{2+} (Fig. 10 and S15–18,† respectively). This emission is characteristic of the rhodamine 6G emission, as a result of the ring opening of the rhodamine derivative. The theoretical fit of the 1 : 1 stoichiometric binding mode of **1** for Ag^{+} gave a log K_s value of 4.34. This value is comparable to that obtained in the electronic absorption titration study, indicating the same reason derived from the ring opening of the rhodamine moiety. Because a substantial amount of the open form of rhodamine 6G was already found in the acetonitrile solution of **4**, relatively small emission spectral changes were observed upon addition of Hg^{2+}, Pb^{2+}, Cu^{2+} and Zn^{2+} to the solution of **4** (Fig. S19–22†). With increasing concentrations of Hg^{2+}, Pb^{2+} and Cu^{2+} in the solution of **7**, a drastic emission enhancement at 560 nm was observed (Fig. S23–25†). The corresponding emission experiment also supported the fact that **10** possesses the highest selectivity. Only Hg^{2+} was able to induce the ring opening process and the emission spectral changes are shown in Fig. 11. Relative to the electronic absorption titration study, a comparable log K_s value of 4.81 was also calculated.

Conclusion

Several classes of rhodamine derivative-containing transition metal complexes, including rhenium(I) tricarbonyl diimine, ruthenium(II) diimine, cyclometallated iridium(III) and rhodium(III) diimine, as well as ruthenium(II) and iridium(III) terpyridine systems, have been synthesized and characterized. The X-ray crystal structure of one cyclometallated rhodium(III) diimine complex (**11**) with a rhodamine substituent was determined. Solution emissions at 546–720 nm were observed for most complexes at room temperature. The complexes with direct connection to the rhodamine moiety, **1**, **4**, **7** and **10**, were found to give sensing responses towards various metal cations, such as Hg^{2+}, Ag^{+}, Pb^{2+}, Cu^{2+} and Zn^{2+} ions. A characteristic absorption band at 530 nm and an emission band at 560 nm were observed due to rhodamine 6G, corresponding to the occurrence of the ring opening process. Binding constants and detection limits were obtained using spectroscopic methods. Depending on the nature of the transition metal centres, chelating ligands as well as the linker to the rhodamine derivative, different sensing properties in terms of selectivity, sensitivity and binding stability, could be deduced.

Acknowledgements

K.M.C.W. acknowledges the receipt of the "Young Thousand Talents Program" award and the start-up fund administrated by the South University of Science and Technology of China. This project was also supported by the National Scientific Foundation of China (grant no. 21471074) and "Peacock Scheme of Innovative Technology in Shenzhen" (grant no. KQCX20140522151005146). M.H.-C.L. acknowledges the receipt of a postgraduate studentship, administered by the University of Hong Kong. We gratefully thank Prof. V.W.W. Yam for access to the equipment for the photophysical measurements.

Notes and references

1 (*a*) C. J. Pedersen, *J. Am. Chem. Soc.*, 1967, **89**, 7017; (*b*) J. M. Lehn, *Struct. Bonding*, 1973, **16**, 1; (*c*) D. J. Cram, T. Kaneda, G. M. Lein and R. C. Helgeson, *J. Chem. Soc., Chem. Commun.*, 1979, 948; (*d*) C. J. Pedersen and J. M. Lehn, *Angew. Chem., Int. Ed. Engl.*, 1988, **27**, 1021; (*e*) D. J. Cram, *Angew. Chem., Int. Ed. Engl.*, 1988, **27**, 1009.

2 (*a*) P. Bühlmann, E. Pretsch and E. Bakker, *Chem. Rev.*, 1998, **98**, 1593; (*b*) D. Diamond and M. A. Mckervey, *Chem. Soc. Rev.*, 1996, 15.

3 (*a*) Y. Inoue and G. W. Gokel, *Cation Binding by Macrocycles*, Marcel Dekker, New York, 1990; (*b*) G. W. Gokel, *Crown Ethers and Cryptands*, Royal Society of Chemistry, Cambridge, 1994; (*c*) R. M. Izatt, L. D. Hansen, D. J. Eatough, J. S. Bradshaw and J. J. Christensen, in *Metal–Ligand Interactions in Organic Chemistry and Biochemistry*, ed. B. Pullman and N. Goldblum, Reidel, Dordrecht, 1997, Part I, p. 337.

4 V. Dujols, F. Ford and A. W. Czarnik, *J. Am. Chem. Soc.*, 1997, **119**, 7386.

5 (*a*) D. T. Quang and J. S. Kim, *Chem. Rev.*, 2010, **110**, 6280; (*b*) J. S. Kim and D. T. Quang, *Chem. Rev.*, 2007, **107**, 3780; (*c*) E. M. Nolan and S. Lippard, *J. Chem. Rev.*, 2008, **108**, 3443; (*d*) X. Chen, Y. Zhou, X. Peng and J. Yoon, *Chem. Soc. Rev.*, 2010, **39**, 2120; (*e*) Y. Zhou, Z. Xu and J. Yoon, *Chem. Soc. Rev.*, 2011, **40**, 2222; (*f*) H. N. Kim, Z. Guo, W. Zhu, J. Yoon and H. Tian, *Chem. Soc. Rev.*, 2011, **40**, 79; (*g*) Z. Xu, S. K. Kim and J. Yoon, *Chem. Soc. Rev.*, 2010, **39**, 1457; (*h*) R. Martinez-Manez and F. Sancenon, *Chem. Rev.*, 2003, **103**, 4419; (*i*) X. Chen, X. Tian, I. Shin and J. Yoon, *Chem. Soc. Rev.*, 2011, **40**, 4783.

6 (*a*) H. Zheng, Z.-H. Qian, L. Xu, F.-F. Yuan, L.-D. Lan and J.-G. Xu, *Org. Lett.*, 2006, **8**, 859; (*b*) M. H. Lee, S. J. Lee, J. H. Jung, H. Lim and J. S. Kim, *Tetrahedron*, 2007, **63**, 12087; (*c*) J. H. Soh, K. M. K. Swamy, S. K. Kim, S. Kim, S. H. Lee and J. Yoon, *Tetrahedron Lett.*, 2007, **48**, 5966; (*d*) J.-S. Wu, I.-C. Hwang, K. S. Kim and J. S. Kim, *Org. Lett.*, 2007, **9**, 907; (*e*) M. G. Choi, D. H. Ryu, H. L. Jeon, S. Cha, J. Cho, H. H. Joo, K. S. Hong, C. Lee, S. Ahn and S.-K. Chang, *Org. Lett.*, 2008, **10**, 3717.

7 (*a*) D. Wu, W. Huang, C. Duan, Z. Lin and Q. Meng, *Inorg. Chem.*, 2007, **46**, 1538; (*b*) M. Suresh, A. Shrivastav, S. Mishra, E. Suresh and A. Das, *Org. Lett.*, 2008, **10**, 3013; (*c*) X. Zhang, Y. Shiraishi and T. Hirai, *Tetrahedron Lett.*, 2007, **48**, 5455; (*d*) J. Mao, L. Wang, W. Dou, X. Tang, Y. Yan and W. Liu, *Org. Lett.*, 2007, **9**, 4567; (*e*) J. Atanu, J. S. Kim, H. S. Jung and K. B. Parimal, *Chem. Commun.*, 2009, 4417.

8 (*a*) C. Wang and K. M. C. Wong, *Inorg. Chem.*, 2011, **50**, 5333; (*b*) C. Wang and K. M. C. Wong, *Inorg. Chem.*, 2013, **52**, 13432; (*c*) K. M. C. Wong, C. Wang, H. C. Lam and N. Zhu, *Polyhedron*, 2015, **86**, 133.

9 (*a*) M. Zhang, Y. Gao, M. Li, M. Yu, F. Li, L. Li, M. Zhu, J. Zhang, T. Yi and C. Huang, *Tetrahedron Lett.*, 2007, **48**, 3709; (*b*) S. Bae and J. Tae, *Tetrahedron Lett.*, 2007, **48**, 5389; (*c*) X. Zhang, Y. Shiraishi and T. Hirai, *Tetrahedron Lett.*, 2008, **49**, 4178.

10 (*a*) Y. Xiang, A. Tong, P. Jin and Y. Ju, *Org. Lett.*, 2006, **8**, 2863; (*b*) M. H. Lee, H. J. Kim, S. Yoon, N. Park and J. S. Kim, *Org. Lett.*, 2008, **10**, 213.

11 K. Huang, H. Yang, Z. Zhou, M. Yu, F. Li, Z. Gao, T. Yi and C. Huang, *Org. Lett.*, 2008, **10**, 2557.

12 S. Subhankar, K. Dokyoung, S. Hyewon, W. C. Seo and H. A. Kyo, *Chem. Soc. Rev.*, 2015, DOI: 10.1039/c4cs00328d, in press, and references herein.

13 (*a*) R. M. Franzini and E. T. Kool, *Org. Lett.*, 2008, **10**, 2935; (*b*) X. Chen and J. Zou, *Microchim. Acta*, 2007, **157**, 133; (*c*) X.-F. Yang, X.-Q. Guo and Y.-B. Zhao, *Talanta*, 2002, **57**, 883; (*d*) H. Zheng, G.-Q. Shang, S.-Y. Yang, X. Gao and J.-G. Xu, *Org. Lett.*, 2008, **10**, 2357; (*e*) S. Kenmoku, Y. Urano, H. Kojima and T. Nagano, *J. Am. Chem. Soc.*, 2007, **129**, 7313.

14 (*a*) E. Baranoff, I. M. Dixon, J. P. Collin, J. P. Sauvage, B. Ventura and L. Flamigni, *Inorg. Chem.*, 2004, **43**, 3057; (*b*) V.-M. Mukkala, M. Helenius, I. Hemmilä, J. Kankare and H. Takalo, *Helv. Chim. Acta*, 1993, **76**, 1361.

15 S. K. Sprouses, K. A. King, P. J. Spellane and R. J. Watts, *J. Am. Chem. Soc.*, 1984, **106**, 6647.

16 (*a*) M. Nonoyama and K. Yamasaki, *Inorg. Nucl. Chem. Lett.*, 1971, **7**, 943.

17 B. P. Sullivan, D. J. Salmon and T. J. Meyer, *Inorg. Chem.*, 1978, **17**, 3334.

18 P. A. Adcock, F. R. Keene, R. S. Smythe and M. R. Snow, *Inorg. Chem.*, 1984, **23**, 2336.

19 J. P. Collin, I. M. Dixon, J. P. Sauvage, J. A. G. Williams, F. Barigelletti and L. Flamigni, *J. Am. Chem. Soc.*, 1999, **121**, 5009.

20 R. N. Dominey, B. Hauser, J. Hubbard and J. Dunham, *Inorg. Chem.*, 1991, **30**, 4754.

21 (*a*) V. W. W. Yam, K. M. C. Wong, V. W. M. Lee, K. K. W. Lo and K. K. Cheung, *Organometallics*, 1995, **14**, 4034. K. M. C. Wong, W. P. Li, K. K. Cheung and V. W. W. Yam, *New J. Chem.*, 2005, **29**, 165.

22 E. Amouyal, A. Homsi, J. C. Chambron and J. P. Sauvage, *J. Chem. Soc., Dalton Trans.*, 1990, 1841.
23 R. V. Kiran, C. F. Hogan, B. D. James and D. J. D. Wilson, *Eur. J. Inorg. Chem.*, 2011, **2011**, 4816.
24 K. K. W. Lo, C. K. Li, K. W. Lau and N. Zhu, *Dalton Trans.*, 2003, 1841.
25 K. K. W. Lo, C. K. Chung, D. C. M. Ng and N. Zhu, *New J. Chem.*, 2002, **26**, 81.
26 (*a*) E. C. Constable, M. D. Ward and S. Corr, *Inorg. Chim. Acta*, 1988, **141**, 201; (*b*) V. W. W. Yam and V. W. M. Lee, *J. Chem. Soc., Dalton Trans.*, 1997, 3005.
27 J. Bourson, J. Pouget and B. Valeur, *J. Phys. Chem.*, 1993, **97**, 4552.
28 SHELXS97: G. M. Sheldrick, *SHELX97. Programs for Crystal Structure Analysis (Release 97-2)*, University of Goetingen, Germany, 1997.
29 SHELXL97: G. M. Sheldrick, *SHELX97. Programs for Crystal Structure Analysis (Release 97-2)*, University of Goetingen, Germany, 1997.
30 K. K. W. Lo, C. K. Chung and N. Zhu, *Chem. – Eur. J.*, 2006, **12**, 1500.
31 K. K. W. Lo and T. K. M. Lee, *Inorg. Chem.*, 2004, **43**, 5275.